2012 IEEE International Conference on Control Applications (CCA)
Part of 2012 IEEE Multi-Conference on Systems and Control
October 3-5, 2012. Dubrovnik, Croatia

The Integrated Vehicle Longitudinal Control System for ABS and TCS

Kwanghyun Cho[1], Jinsung Kim[1], and Seibum Choi[2],

Abstract— **This paper proposes the vehicle longitudinal controller for the Anti-lock Braking System(ABS) and Traction Control System(TCS). The sliding mode control scheme without a sign function is used to design a controller. Instead of a sign function, the adaptation mechanism is used to reduce the actuator chattering as a problem of the sliding mode control. The proposed systems use the equivalent model from engine to wheel to control the brake and engine actuator. Using the integrated logic frame, it reduces the computation load of Electrical Control Unit(ECU) equipped on the vehicle and make integrating a variety of vehicle stability controllers such as ABS, TCS, and ESC(Electronic Stability Control) more easily. The proposed systems are made up of three sub-systems, which are the vehicle state estimator, vehicle state controller and vehicle actuator controller. The performance of the proposed system is verified with a variety of standard ABS and TCS test conditions using the CarSim.**

I. INTRODUCTION

In these days, a variety of the vehicle stability control systems have been developed for the safety of a vehicle. These systems are classified by the vehicle motion such as the longitudinal, lateral and vertical direction. Especially, the vehicle longitudinal control systems such as an Anti-lock Braking System(ABS) and Traction Control System(TCS) had been developed first, which have been equipped with most vehicle widely. Both systems operate under the opposite conditions. The ABS controller is applied to prevent four wheels from locking when the vehicle is decelerating heavily, which uses four brake actuators. In case that the vehicle is accelerating heavily, the TCS is operated to prevent the driven wheel from occurring the over-slip, which uses the driven wheel brake actuators and an engine actuator. Therefore, it is not easy to integrate both systems under only one logic frame and the complicated algorithm structure may consist of lot of memory.

Many researches of both systems have been performed and a variety of the control schemes have been used. However, most studies assume that the optimal control target(desires wheel slip or wheel speed) is known. [1][2] These systems have focused on only how the measurements such as wheel slip or speed track the desired value well.[3][4][5] Actually, it is difficult to define the control target exactly under a variety of road conditions because the road friction coefficient is unknown and it is impossible to measure it by using only equipped sensors such as an yaw rate sensor and accelerometers. Therefore, the control problem only considered the perfect tracking (asymptotically stable) is meaningless.

*This work was supported by Hyundai Motors

[1]K. Cho and J. Kim are with the Department of Mechanical Engineering, KAIST, 335 Gwahak-ro (373-1 Guseong-dong), Yuseong-gu, Daejeon, 305-701, Republic of Korea khcho08@kaist.ac.kr, jsk@kaist.ac.kr

[2]S.B. Choi is with the faculty of the Department of Mechanical Engineering, KAIST, 335 Gwahak-ro (373-1 Guseong-dong), Yuseong-gu, Daejeon, 305-701, Republic of Korea sbchoi@kaist.ac.kr

This study proposes the integrated longitudinal vehicle control system. The equivalent dynamics from engine to wheel is used to design adaptive PID control scheme. It makes the integration of both systems more easily because the actuator controllers are designed by this model. Therefore, it can reduce the computation load of ECU equipped on the vehicle and algorithm complexity. The proposed systems are made up of three sub-systems, which are the vehicle state estimator, vehicle state controller, and vehicle actuator controller. The road friction coefficient is calculated to obtain the control target such as the desired wheel and engine speed.

The paper is organized as follows: In Section II, the vehicle states such as the normal force, brake torque and road friction coefficient are calculated by physical dynamics. In Section III and V, the vehicle state controllers and vehicle actuator controller are presented to obtain the desired control targets and to control brake and engine actuators. The simulation results are shown in Section V to verify the performance of the proposed system. Concluding remarks are given in Section VI.

II. VEHICLE STATE ESTIMATOR

In this section, the normal forces and brake torques are calculated by physical dynamics. Four wheel pressure sensors, which have been used for a regenerative braking system in the hybrid vehicles or an ACC(adaptive cruise control) system recently, are used to measure wheel pressure signals. Using the wheel dynamics based on these parameters, the road friction coefficient is obtained. And the driveline dynamics are described for the brake and engine control model.[6]

A. Normal Force Computation

The normal forces of the vehicle are calculated by the longitudinal vehicle dynamcis, which is described in Fig. 1. The normal forces of front and rear wheels are calculated as follows:

$$F_{zf} = \frac{mgl_r cos\theta - mghsin\theta + m\ddot{x}h - F_{aero}h_{aero}}{L} \quad (1)$$

$$F_{zr} = \frac{mgl_f cos\theta + mghsin\theta + m\ddot{x}h + F_{aero}h_{aero}}{L} \quad (2)$$

where, F_{zf} and F_{zr} are the normal forces of the vehicle, m the total vehicle mass, l_f and l_r the distance from C.G. to front and rear wheel, L the wheel base length, g the gravity acceleration, θ the road elevation, h the height of C.G, and $F_{aero}h_{aero}$ the moment of aero effect.

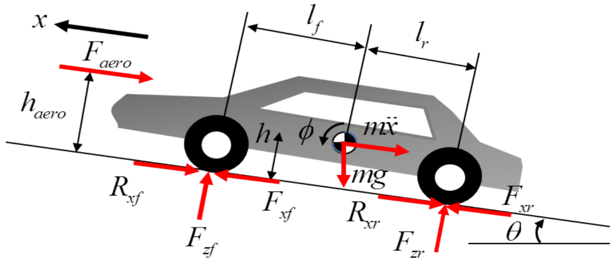

Fig. 1. Vehicle longitudinal dynamics

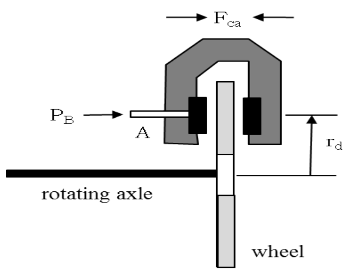

Fig. 2. Relation between force and pressure

When the vehicle is decelerating, the vehicle acceleration assumes the positive value and otherwise negative one. Here, assume that the road surface is flat, i.e., $\theta \approx 0$ and air drag is negligible, i.e., $F_{aero}h_{aero} \approx 0$. Then, (1) and (2) are approximated simply as follows:

$$F_{zf} \approx \frac{mgl_r + m\ddot{x}h}{L} \tag{3}$$

$$F_{zr} \approx \frac{mgl_f + m\ddot{x}h}{L} \tag{4}$$

B. Brake Torque Computation

The brake torques are obtained by the relation between force applied to four wheels and cylinder pressure as described in Fig. 2. The force applied to brake disk pad is obtained as follows,

$$F_B = \mu_b F_{ca} = \mu_b 2F_{BN} = 2\mu_b P_B A \tag{5}$$

where, F_B is the brake force, μ_b the caliper friction coefficient, F_{ca} the clamping force, F_{BN} the normal brake force, P_B the brake pressure, and A the cylinder area.

The brake torque is computed as follows,

$$T_B = F_B \cdot r_d = k_B P_B \tag{6}$$

where, T_B is the brake torque and r_d the disk radius. k_B represents the brake gain which is determined by the specification of brake cylinder. In this study, the brake gains of front and rear wheels are 200N·m/MPa and 70N·m/MPa.

C. Road Friction Coefficient Computation

The road friction coefficient is calculated by wheel dynamics in Fig. 3. It is usually used for the brake actuator of ABS. The moment balance equation of the wheel is obtained as follows,

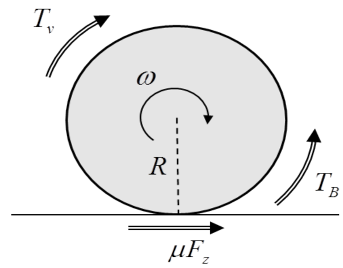

Fig. 3. Wheel dynamics

$$J_w \dot{\omega}_w = T_v - RF_x - T_B \tag{7}$$

where, J_w and ω_w are the wheel inertia and angular speed, R the wheel radius, F_x the longitudinal tire force, T_B the brake torque and T_v the driving torque.

The relation between the longitudinal tire force, F_x and the normal tire force, F_z is represented as follows,

$$F_x = \mu F_z \tag{8}$$

where, μ is the road friction coefficient.

In (7) and (8), the road friction coefficient is obtained by normalizing the longitudinal tire force using the normal tire force. It is presented as follows,

$$\mu = \frac{F_x}{F_z} = \frac{T_v - J_w \dot{\omega} - T_B}{RF_z} \tag{9}$$

The μ obtained in (9) oscillates in accordance with wheel cycling pattern caused by the braking operation such as apply-hold-dump in ABS. Therefore, it must be limited by a rate limiter to obtain the maximum road friction coefficient. The applied rate limiter is as follows:

$$\mu_{peak} = \begin{cases} \mu + \dot{\mu}_{max} \cdot T_s & if \quad \dot{\mu} \geqq \dot{\mu}_{max} \\ \mu - \dot{\mu}_{min} \cdot T_s & elseif \quad \dot{\mu} < \dot{\mu}_{min} \\ \mu & otherwise \end{cases} \tag{10}$$

where, $\dot{\mu}_{max}$ and $\dot{\mu}_{min}$ are the maximum and minimum rate limitation of μ, and T_s is the sampling time.

The maximum friction coefficient, μ_{peak}, means the maximum braking force obtained during the braking. It is used to obtain the control targets of the rear wheels in ABS. It can improve the implementation problem that the control target is unknown indirectly. Also, it enables all wheels to be controlled under each estimated road friction coefficient. Therefore, it can guarantee the lateral stability of the vehicle on the split friction road condition or curve braking.

D. Driveline Model

The driveline model provides useful dynamics to design the brake and engine controller. The engine can be controlled in point of wheels and wheels can also be controlled on the contrary to this. Therefore, this is applied easily to the brake and engine actuator control in ABS and TCS. The driveline model is described in Fig. 4. For simplicity, the transient characteristics and the damping effects of clutch and transmission are ignored. [7]

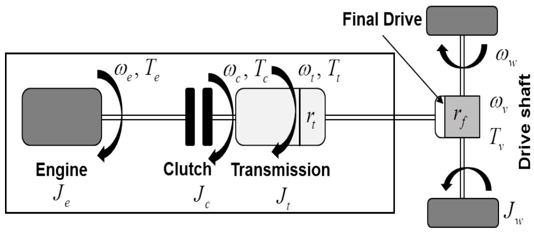

Fig. 4. Driveline dynamics model

In Fig. 4, the moment balance equations from engine to drive shaft are obtained as follows,

$$J_e \dot{\omega}_e = T_e - T_c \tag{11}$$

$$J_c \dot{\omega}_c = T_c - T_t \tag{12}$$

$$J_t \dot{\omega}_t = T_t - \frac{T_v}{r_t r_f} \tag{13}$$

$$J_v \dot{\omega}_v = T_v - T_L \tag{14}$$

where, J_e, ω_e and T_e are the engine inertia, angular speed and torque, J_c, ω_c, and T_c the clutch inertia, angular speed and torque, J_t, ω_t and T_t the transmission inertia, angular speed and torque. r_t the transmission gear ration, r_f the final gear ration, and T_L the load torque. Here, J_v and ω_v are defined as follows,

$$J_v = 2J_w, \quad \omega_v = \frac{\omega_{wL} + \omega_{wR}}{2}$$

where, ω_{wL} and ω_{wR} are angular speed of left and right side wheel.

When it assumes that the vehicle is on the steady-state, the angular speed of the engine, clutch and transmission become equally.

$$\omega_e \approx \omega_c \approx \omega_t \tag{15}$$

However, the angular speed between transmission and drive shaft is different because of the gear ratio of transmission and final drive.

$$\omega_t = r_t r_f \omega_v \tag{16}$$

Therefore, the dynamics on the drive shaft is obtained by substituting (7), and (11) ∼(13) into (14) as follows,

$$\left\{ (J_e + J_c + J_t)(r_t r_f) + \frac{J_v}{r_t r_f} \right\} \dot{\omega}_v = T_e - \frac{\sum T_B}{r_t r_f} - \frac{R \sum F_x}{r_t r_f} \tag{17}$$

where, $\sum T_B$ is the sum of left and right brake torque, and $\sum F_x$ the sum of left and right longitudinal tire force.

(17) is the equivalent model from engine to drive shaft to control the engine torque. In case of the brake control, the reference of the equivalent mode must be changed from a drive shaft to each wheel as follows,

$$\left\{ \frac{(J_e + J_c + J_t)(r_t r_f)^2}{2} + J_w \right\} \dot{\omega}_w = \frac{r_t r_f}{2} T_e - T_B - R F_x \tag{18}$$

III. VEHICLE STATE CONTROLLER

In this section, it is described how the control targets are obtained. And the rear wheel control scheme of ABS is introduced to describe how to obtain the control target of the front wheel because the front wheels are controlled by the wheel speed obtained from the controlled rear wheel.

A. Anti-lock Brake System

1) Rear Wheel Control: The rear wheels are controlled by wheel acceleration based rules. The desired acceleration is obtained from (10), and the error between measured and desired acceleration is also used as a feedback term. It works like a P-type controller. Therefore, the rear wheel brake system is considered as a semi-feedback one. The valve command to control rear wheels is presented as sum of valve dump command and valve apply command as follows:

$$V_{cmd} = V_{dump} \cdot V_{dhold} + V_{apply} \cdot V_{ahold} \tag{19}$$

where, V_{cmd} is the total valve command, V_{dump} valve dump command, V_{apply} valve apply command, V_{dhold} valve hold command for dump, and V_{ahold} valve hold command for apply.

The dump and apply valve commands are obtained by the difference between estimated wheel acceleration and reference wheel acceleration. The commands for valve dump and apply are represented as follows:

$$V_{dump} = \begin{cases} a_w - a_{dump} & if \quad a_w - a_{dump} < 0 \\ 0 & otherwise \end{cases} \tag{20}$$

$$V_{apply} = \begin{cases} a_w - a_{apply} & if \quad a_w - a_{apply} > 0 \\ 0 & otherwise \end{cases} \tag{21}$$

where, a_w is estimated wheel acceleration, a_{dump} reference acceleration for dump, and a_{apply} reference acceleration for apply.

The reference accelerations, a_{dump} and a_{apply}, are obtained from the calculated maximum road friction coefficient, μ_{max} with additional margin. For example, the reference accelerations, a_{dump} and a_{apply} are determined as follows:

$$a_{dump} = -1 \cdot [|a_{max}| \cdot 1.20 + 0.7 \cdot g] \tag{22}$$

$$a_{apply} = -1 \cdot [|a_{max}| \cdot 1.05 + 0.1 \cdot g] \tag{23}$$

where, a_{max} means the maximum acceleration during braking on the driving road using the road friction coefficient estimated in (10).

$$a_{max} = \mu_{peak} \cdot g \tag{24}$$

The valve hold commands determine whether the valve dump/apply commands are applied or not. The commands of the valve hold are as follows:

$$V_{dhold} = \begin{cases} 0 & if \quad |V_{dump}| < V_{holdth} \quad for \quad t < t_1 \\ 1 & otherwise \end{cases} \tag{25}$$

$$V_{ahold} = \begin{cases} 0 & if \quad V_{apply} > 0 \quad for \quad t < t_2 \\ 1 & otherwise \end{cases} \tag{26}$$

where, V_{holdth} is a threshold for dump hold, t_1 a time threshold to keep small dump command, t_2 a time threshold to be ready to start apply command.

The apply-hold-dump commands make cycling patterns of the rear wheels around the peak friction slip point.

2) Front Wheel Control: The front wheels have no direct cycling patterns like rear wheels because it makes the ride very harsh on high-friction surfaces. The target speeds of front wheels are obtained from controlled rear wheel speed with additional slip margin. The validity of the control target is guaranteed by an assumption that the rear wheels are controlled near a peak friction point through a cycling-pattern. The desired wheel speed, ω_{Fwdes}, is represented as follows,

$$\omega_{Fwdes} = \omega_{Rw} + \Delta\omega \tag{27}$$

where ω_{Rw} is rear wheel speed, $\Delta\omega$ additional slip margin.

B. Traction Control System

The objective of TCS is to prevent the driven wheels from occurring over-slip by heavy acceleration. Therefore, average speed of undriven wheels with slip margin becomes the desired control target of driven wheels. However, the desired wheel speed(control target) of brake and engine actuator must be different because two actuators may be operated very frequently. This study proposes that the desired wheel speed of the brake control becomes higher than one of the engine control as follows,

- Brake Control

$$\omega_{Fwdes} = \omega_{Rw-average} + \Delta\omega + 1 \tag{28}$$

- Engine Control

$$\omega_{vdes} = \omega_{Rw-average} + \Delta\omega \tag{29}$$

where $\omega_{Rw-average}$ is the average speed of two rear wheels and $\Delta\omega$ additional slip margin.

The slip margin in this study is about 10% of the un-driven wheel speed. It is determined by a variety of actual experiments.

IV. VEHICLE ACTUATOR CONTROLLER

In this section, the brake control schemes of front wheels in ABS and driven wheels in TCS are presented. In case of front-wheel driven vehicle, the brake control logics of ABS and TCS are same. And the engine torque control scheme in TCS is presented.

A. Brake Controller

The controllers of the brake actuators are designed by (18). The rearrange of (18) is represented as follows,

$$\dot{\omega}_w = \frac{r_t r_f}{2J_{wb}} T_e - \frac{T_B}{J_{wb}} - \mu \frac{RF_z}{J_{wb}} \tag{30}$$

where,

$$J_{wb} = \frac{(J_e + J_c + J_t)(r_t r_f)^2}{2} + J_w$$

In (30), the change rate of brake torque is proportional to fluid flow rate, and flow rate is proportional to control valve opening. Therefore, the brake torque rate is proportional to the valve command and then it becomes the control input.[8] Using (30), the system model to design the controller is defined as follows:

$$\ddot{\omega}_w = -\frac{1}{J_{wb}} \dot{T}_B + d \tag{31}$$

where,

$$d = \frac{r_t r_f}{2J_{wb}} \dot{T}_e - \frac{1}{J_{wb}} \frac{d}{dt}(\mu R F_z)$$

The control objective is to track the desired wheel speed, ω_{Fwdes}. In this study, the PID controller is proposed and the adaptation mechanism of the disturbance, d is designed. In case that the information of d is totally unknown, the adaptation mechanism does not work well because of the fast time-varying characteristic of parameter derivative. This makes the tracking performance very poor. However, it can be improved because the nominal value of d, d_n can be calculated by using (3) and (9) in this study. Therefore, (31) is rewritten as follows:

$$\ddot{\omega}_w = -\frac{1}{J_{wb}} \dot{T}_B + d_n + \Delta d \tag{32}$$

Here, $\Delta d = d - d_n$ is the error between the actual disturbance and the nominal disturbance. To design the adaptive controller, the PID type error dynamics is defined as follows,

$$S_b = \dot{e}_b + 2\zeta\lambda_b e_b + \lambda_b^2 \int e_b dt, \qquad \zeta > 0, \quad \lambda_b > 0 \tag{33}$$

where, $e_b = \omega_w - \omega_{Fwdes}$ is the tracking error, and ζ, λ_b the tuning parameters.

This study uses the sliding mode control scheme without sign function to reduce the actuator chattering. The aim of the sliding mode control is to force the system state to the sliding surface $S = 0$ and then maintain it on the sliding surface. Therefore, the sliding surface, S must satisfy,

$$\dot{S}_b \cdot S_b \leq 0 \tag{34}$$

And, (34) can be satisfied using (35)

$$\dot{S}_b = -K_{be} S_b, \qquad K_{be} > 0 \tag{35}$$

From (35), the control law is obtained as follows,

$$\dot{T}_B = u_b = J_{wb}\Big(-\ddot{\omega}_d + 2\zeta\lambda_b \dot{e}_b + \lambda_b^2 e_b + K_{be} S_b + d_n + \Delta\hat{d} \Big) \tag{36}$$

Here, the disturbance error $\Delta\hat{d}$ must be estimated by using the adaptation mechanism. The adaptation law is designed as follows:

$$\Delta\dot{\hat{d}} = K_{ba}\big(\dot{e}_b + 2\zeta\lambda_b e_b + \lambda_b^2 \int e_b dt\big), \qquad K_{ba} > 0 \tag{37}$$

where, K_{ba} is the tuning parameter of the adaptation algorithm.

The control law (36) and the adaptation law (37) gurantee the stability of the system. Let's define a Lyapunov function,

$$V = \frac{1}{2} S_b^2 + \frac{1}{2K_{ba}} (\Delta d - \Delta\hat{d})^2 > 0, \qquad K_{ba} > 0 \tag{38}$$

The derivative of (38) is as follows:

$$\dot{V} = S_b \dot{S}_b + \frac{1}{K_{ba}}(\Delta d - \Delta \hat{d})(\Delta \dot{d} - \Delta \dot{\hat{d}}) \tag{39}$$

The disturbance error, Δd assumes that it is varying slowly because the nominal value, d_n is tracking the actual disturbance, d. Therefore, Δd is considered as a constant and the derivative of Δd is nearly equal to zero, i.e., $\Delta \dot{d} \approx 0$ and (39) is recalculated using (33), (36) and (37) as follows:

$$\dot{V} = S_b \dot{S}_b - \frac{1}{K_{ba}}(\Delta d - \Delta \hat{d})\Delta \dot{\hat{d}} = -K_{be} S_b^2 \leq 0 \tag{40}$$

Therefore, it is proved that the system is stable. Using LaSalle's invarient set theorem, the asymptotical stability of the system is also proved. If $e_b = 0$, only $e_b = 0$ makes $S_b = 0$ in (33) and $S_b = 0$ makes $\dot{S}_b$ = 0. Substituting (36) into (32), above relation makes $\Delta d - \Delta \hat{d}$ = 0. Therefore, the equilibrium point e_b, $\dot{e}_b$ and $\Delta d - \Delta \hat{d}$ are asymptotically stable.

B. Engine Controller

In this study, the equivalent model from engine to drive shaft, (17), is used to control the engine actuator. Rewriting (17),

$$\dot{\omega}_v = \frac{1}{\mathbf{J}_{we}} T_e - \frac{1}{\mathbf{J}_{we}} \frac{1}{r_t r_f} \mathbf{T}_B - \frac{1}{\mathbf{J}_{we}} \frac{R}{r_t r_f} \mathbf{F}_x \tag{41}$$

where,

$$\mathbf{J}_{we} = (J_e + J_c + J_t)(r_t r_f) + \frac{2J_w}{r_t r_f},$$

$$\mathbf{T}_B = T_{BL} + T_{BR}, \quad \mathbf{F_x} = F_{xL} + F_{xR}$$

Here, the control input is the engine torque, T_e. The control objective is to track the desired engine speed, ω_{vdes}. As shown in the brake controller, the PI controller is proposed and the adaptation mechanism of the longitudinal tire force, $\mathbf{F}_x$ is designed.

To design the adaptive controller, the PI type error dynamics is defined as follows,

$$S_e = e_e + \lambda_e \int e_e dt, \qquad \lambda_e > 0 \tag{42}$$

where, $e_e = \omega_v - \omega_{vdes}$ is the tracking error, ω_{vdes} the desired engine speed, and λ_e the tuning parameters.

As shown in the brake controller, the sliding mode control scheme without sign function is used. Therefore, the sliding surface, S_e must satisfy,

$$\dot{S}_e \cdot S_e \leq 0 \tag{43}$$

And, (34) can be satisfied using (35)

$$\dot{S}_e = -K_{ee} S_e, \qquad K_{ee} > 0 \tag{44}$$

From (44), the control law is obtained as follows,

$$T_e = u_e = J_{we} \dot{\omega}_{vdes} + \frac{\mathbf{T}_B}{r_t r_f} + R \frac{\hat{\mathbf{F}}_x}{r_t r_f} - K_{ee} S_e \tag{45}$$

Here, the longitudinal tire force, $\hat{\mathbf{F}}_x$ is estimated by the adaptive law as follows:

$$\dot{\hat{\mathbf{F}}}_x = -\frac{K_{ea}}{\mathbf{J}_{we}} \frac{R}{r_t r_f} \left(e + \lambda_e \int edt\right) \tag{46}$$

TABLE I

SIMULATION CASE SCENARIO

Case1(TCS)	Full accel	high(μ=0.8) to low(μ=0.3)
Case2(ABS)	100kph	high(μ=0.8) to low(μ=0.2)
Case3(ABS)	100kph	high(μ=0.8) to low(μ=0.2)

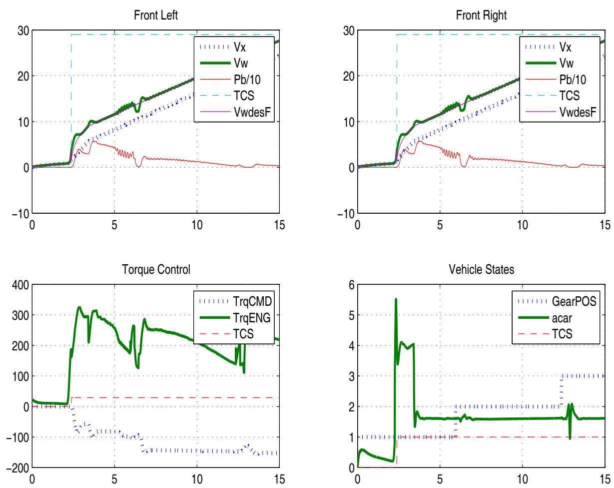

Fig. 5. Case1. High To Low: TCS

where, K_{ea} is the tuning parameter of the adaptation algorithm.

The control law (45) and the adaptation law (46) gurantee the stability of the system. Let's define a Lyapunov function,

$$V = \frac{1}{2} S_e^2 + \frac{1}{2K_{ea}} (\mathbf{F}_x - \hat{\mathbf{F}}_x)^2 > 0, \qquad K_{ea} > 0 \tag{47}$$

The derivative of (47) is as follows:

$$\dot{V} = S_e \dot{S}_e + \frac{1}{K_{ea}} (\mathbf{F}_x - \hat{\mathbf{F}}_x)(\dot{\mathbf{F}}_x - \dot{\hat{\mathbf{F}}}_x) \tag{48}$$

The derivative of $\mathbf{F}_x$ is nearly equal to zero, i.e., $\dot{\hat{\mathbf{F}}} \approx 0$ and (48) is recalculated by using (42), (45) and (46) as follows:

$$\dot{V} = S\dot{S} - \frac{1}{K_{ba}}(\Delta d - \Delta \hat{d})\Delta \dot{\hat{d}} = -K_{be} S^2 \leq 0 \tag{49}$$

Therefore, it proves that the system is stable. Using LaSalle's invarient set theorem, the asymptotical stability of the system is also proved.

V. SIMULATION

A variety of simulations have been performed to verify the performance of the proposed ABS and TCS algorithm under a lot of conditions using CarSim program. The simulation conditions are standard test conditions of ABS and TCS. In a variety of simulations, the driving scenarios on the mu transition(high to low mu) road are shown in this study. It is shown in TABLE I. These scenarios can show overall performance of designed vehicle state estimator, vehicle state controller, and vehicle actuator controller simultaneously. In

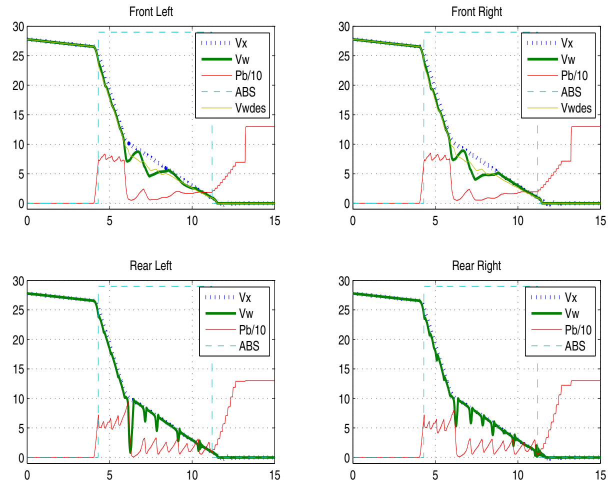

Fig. 6. Case2. High To Low: without Pressure Sensors for ABS

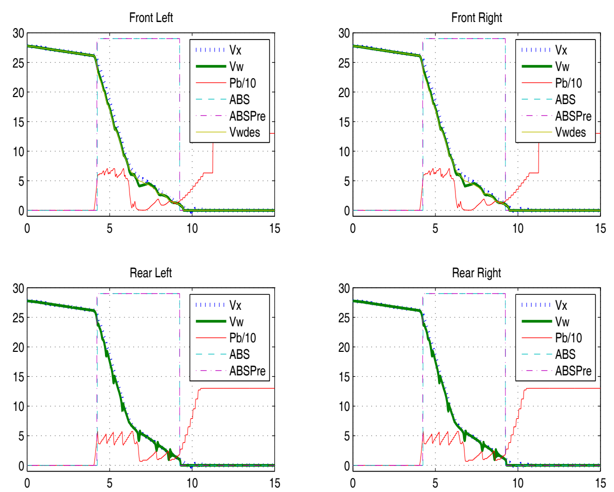

Fig. 7. Case3. High To Low: with Pressure Sensors for ABS

Fig. 5, the road friction coefficient changes from 0.8 to 0.3 at 3.5sec. In spite of sudden mu transition, there is no over-slip for each wheel. Also, the vehicle keeps maximum longitudinal tire force as shown in vehicle acceleration. Fig. 6 and 7 show the effect of using wheel pressure sensors, which means whether the nominal disturbance is known or not in (32). In both figures, the road friction coefficient changes from 0.8 to 0.2 at 6.1sec. And, wheel slip of left and right-side wheels are not same because the C.G point of the vehicle is not in the center of the vehicle. In case of the algorithm without wheel pressure sensors(Fig. 6), the road friction coefficient cannot be estimated, so the detection of the friction variation such as friction transition can be slow or cannot be detected properly. At the moment changing the road friction coefficient from high to low in Fig 6 and 7, the proposed algorithm(Fig. 7) shows that the wheel slip is smaller than that of the algorithm without pressure sensors because of fast detection of surface transition. Therefore, the proposed algorithm shows good performance though sudden mu transition occurs.

VI. CONCLUSIONS

In this study, the integrated longitudinal vehicle controller has been proposed for ABS and TCS. The equivalent dynamics from engine to wheels is used to control the brake and engine actuator, which makes integration of both systems more easily. Also, the sliding mode control scheme is used to design the adaptive controller. However, the sign function has been eliminated to reduce the actuator chattering because it makes the rideability and comfortability of passengers be worse. In stead of, the adaptive mechanics are used to reduce the effect of disturbance and model uncertainties. In the future, a variety of experiments have to be performed to verify the robustness and performance in actual driving conditions.

APPENDIX

The units of legends of Fig. 5∼7 are as follows:

- Vx, Vw, Vwdes, VwdesF: m/s
- acar: m/s^2
- Pb/10: 10bar
- TrqCMD, TrqENG: Nm

ACKNOWLEDGMENT

The research of this paper was supported by Hyundai Motors, Korea. Also, it was supported by the National Research Foundation of Korea (NRF) grant funded by the Korea government(MEST) (No.2012-0000991).

REFERENCES

[1] S. Savaresi, M. Tanelli, and C. Cantoni, "Mixed Slip-Deceleration Control in Automotive Braking Systems", *Journal of Dynamic system, Measurement, and Control*, vol.129. pp 20-31, 2007.

[2] SAE, "Antilock Brake System Review", *Society of Automotive Engineers*, pp 90-102, 1992.

[3] I. Petersen, and et. al, "Wheel Slip Control in ABS Brakes Using GAin Scheduled Constrained LQR", *European Control Conference*, pp 146-155 , 2001

[4] K. Buckholtz, "Reference Input Wheel Slip Trakcing Using Sliding Mode Control", *Society of Automotive Engineers*, no. 2002-01-0301, 2002

[5] T. Johansen, and et. al, "Gain-scheduled Wheel Slip Control in Automotive Brake Systems", *IEEE Trans. on Control System Technology*, vol. 11, no. 6, pp 799-811, 2003

[6] K. Cho, et. al., "Design of an ABS Control Algorithm Using Wheel Dynamics", *Korean Society of Automotive Engineers 2010 Annual Conference*, pp 1756-1761, 2010.

[7] J. Kim and S. Choi, "Vehicle Driveline Modeling and Dynamic Simulation Method", *KSAE 2009 Annual Conference*, pp 1457-1468, 2009.

[8] S. Choi, "Antilock Brake System With a Continuous Wheel Slip Control to Maximize the Braking Performance and the Ride Quality", *IEEE Trans. on Control Systems Technology*, vol. 16, no. 5, pp 996-1003, 2002.